

## RESEARCH NOTE

**A Gaussian Approach to Neural Nets with Multiple Memory Domains**

E. FOURNOU, P. ARGYRAKIS, B. KARGAS &amp; P. A. ANNINOS

*(Received for publication November 1993; revised paper accepted April 1995)*

*Non-isolated randomly interconnected neural nets with chemical markers are investigated, which receive steady or slowly varying excitatory or inhibitory inputs. We extend here our previous studies to include nets of Poisson and Gaussian connectivities. Our results show that the multi-hysteresis loops obtained by applying the steady-state condition for the Gaussian approximation are wider than the corresponding ones of the Poisson case, and they have been slightly shifted to larger values of the parameter  $\sigma^+$  (which is the fraction of external active fibres). Also, in the Gaussian nets, the stable steady states are lower than the corresponding ones of the Poisson nets, whereas the unstable states are higher.*

KEYWORDS: Neural modelling, neural connectivities, chemical markers.

**1. Introduction**

In previous studies (Fournou *et al.*, 1993), we investigated the dynamical behaviour of isolated neural nets with chemical markers and high interneuronal connectivities and the relationship between structure, as expressed in patterns of interneuronal synaptic connectivity, and 'spontaneous' activity. We extend here this investigation to non-isolated netlets with markers. It is assumed that the netlet under consideration is attached to a cable of afferent fibres receiving through it sustained inputs from another netlet with the same structure.

In constructing models of such neuron assemblies, connectivity among individual elements may be specified to follow a given probability law, maintaining all other parameters constant (Anninos & Elul, 1974). The formalism for non-isolated neural nets with markers characterized by high interneuronal connectivity is introduced and we investigate the steady-state activities and hysteresis effects in relation to the interneuronal connectivities.

E. Fournou and P. Argyrakis, Department of Physics 313-1, University of Thessaloniki, 54006 Thessaloniki, Greece. B. Kargas, Department of Applied Sciences, Technological Education Institution (TEI) of Thessaloniki, 57400 Sindos, Greece. P.A. Anninos, Department of Medical Physics, University of Thraki, 68100 Alexandroupolis, Greece. Permanent address of E. Fournou: Department of Applied Sciences, Technological Education Institution (TEI) of Thessaloniki, 57400 Sindos, Greece.

## 2. The Neural Net Model

### 2.1. Assumptions and Definitions

The basic assumptions of the model are the same as in previous work (Anninos *et al.*, 1970); Anninos & Kokkinidis, 1984). Neural nets are assumed to be constructed of discrete sets of randomly interconnected neurons of similar structure and function, but the neural connections are set up by means of chemical markers carried by the individual cells, according to the theory of neural specificity (Sperry, 1943, 1963; Prestige & Willshaw, 1975). They are established only if both pre- and postsynaptic neurons carry the same marker. Thus, the neural population of the netlet is treated as a set of subpopulations of neurons, each of them characterized by a specific chemical marker. The neurons are bistable elements, as was postulated by McCulloch and Pitts (1943), and operate synchronously at discrete times.

In this model, a neural net with  $N$  markers is assumed to be constructed of  $A$  formal neurons. A fraction  $h$  ( $0 < h < 1$ ) of them are inhibitory neurons while the rest are excitatory. Each neuron receives, on average,  $\mu^+$  EPSPs (excitatory postsynaptic potentials) and  $\mu^-$  IPSPs (inhibitory postsynaptic potentials). The size of the PSP produced by an excitatory (inhibitory) unit is  $K^+$  ( $K^-$ ). The netlet is attached to a cable of afferent fibres receiving through it sustained inputs from another netlet of  $A_0$  neurons with the same structure. A fraction  $h_0$  ( $0 < h_0 < 1$ ) of them are inhibitory. With  $\mu_0^+$  ( $\mu_0^-$ ), we denote the average number of neurons in each subsystem with which an external excitatory (inhibitory) neuron makes its synaptic connections in the netlet, while  $K_0^+$  ( $K_0^-$ ) are the corresponding strengths of the synaptic coupling coefficients.

The neurons are characterized by the absolute refractory period, the firing threshold  $\theta$  and the synaptic delay  $\tau$ . It is assumed here that the refractory period is greater than the synaptic delay, but less than twice the synaptic delay. A parameter  $r$  for the refractory period may be used, taking, in general, any integer value. For our purposes,  $r$  was given the value  $r=1$  when refractoriness was assumed, and  $r=0$  otherwise. The neural activity is restricted to discrete times, i.e. if a number of neurons fire simultaneously at time  $t$ , then all neural activity resulting from this initial activity will be restricted to times  $t + \tau$ ,  $t + 2\tau, \dots$

### 2.2. Mathematical Formalism

The dynamic variable of interest is the level of activity  $a_n$ , i.e. the fractional number of neurons in the netlet that are active at time  $t = n\tau$ . The expectation value of activity  $\langle a_{n+1} \rangle$  for a netlet of  $A$  neurons with  $N$  markers with or without sustained inputs is given by the equation

$$\langle a_{n+1} \rangle = (1 - a_n) \sum_{j=1}^N m_j P_j \quad (1)$$

where  $m_j$  ( $j = 1, 2, \dots, N$ ) is the fraction of neurons out of the total carrying the  $j$ th marker in the netlet. Obviously,  $m_1 + m_2 + \dots + m_N = 1$ .  $P_j$  is the probability that a neuron of the  $j$ th marker receives a total PSP which exceeds its threshold  $\theta_j$ . With the term total PSPs, we mean the total algebraic sum of PSPs which arrive at the neuron coming both from the netlet itself and from the fibres attached to the netlet which carry sustained inputs. This probability,  $P_j$ , is given as a function of  $a_n$ ,  $m_j$ ,  $\sigma$  (which is the fraction of external active fibres) and  $\theta_j$ , i.e.  $P_j = P_j(a_n, m_j, \sigma, \theta_j)$ . It

may be expressed in terms of Poisson distribution law or any other distribution law (Anninos & Elul, 1974). The factor  $(1 - a_n)$  in this equation is neglected if no refractoriness is assumed.

For the Poisson approximation, the quantity  $P_j$  is given (Anninos & Kokkinidis, 1984) by

$$P_j(a_n, m_j, \sigma, \tau_j) = \sum_{M=0}^{M_{\max,j}} \sum_{I=0}^{I_{\max,j}} \left( 1 - \sum_{L=0}^{\eta'_j-1} P_{L,j} \right) Q_{I,j} R_{M,j} \tag{2}$$

where  $P_{L,j}$ ,  $Q_{I,j}$  and  $R_{M,j}$  are the probabilities that a neuron of the  $j$ th marker will receive  $L$ -PSPs,  $I$ -PSPs and  $M$ -PSPs, respectively, at time  $t = (n + 1) \tau$ . The upper limits  $M_{\max,j}$ ,  $I_{\max,j}$  and  $\eta'_j$  are the total numbers of the external inputs, of the inhibitory inputs and the minimum number of excitatory inputs necessary to trigger a neuron, respectively. Equation (2) results by adding all probabilities for all combinations of thresholds and PSPs that produce firing.

If the average number of active inputs per neuron becomes sufficiently large, the number of PSPs per neuron will follow a Gaussian distribution. In this case, the quantity  $P_j = P_j(a_n, m_j, \sigma, \theta_j)$  is calculated in analogy to our previous studies (Fournou *et al.*, 1993) for isolated neural nets taking into account the external sustained inputs. If  $l_j$  and  $i_j$  are the numbers of EPSPs and IPSPs, respectively, that are inputs to a given neuron of the  $j$ th marker emanating from the netlet itself, and if  $l'_j$ ,  $i'_j$  are the numbers of external EPSPs and IPSPs, respectively, that are inputs to this neuron emanating from the axons, then the total PSP input to a given neuron of the  $j$ th marker at time  $t = (n + 1) \tau$ , will be given by

$$e_{j, n+1} = l_j K^+ + i_j K^- + l'_j K_0^+ + i'_j K_0^- \tag{3}$$

If all the quantities  $l_j$ ,  $i_j$ ,  $l'_j$  and  $i'_j$  are sufficiently large, their distributions may be approximated by normal distributions about their average values  $\bar{l}_j = a_n \mu_j^+$ ,  $(1 - h_j) m_j$ ,  $\bar{i}_j = a_n \mu_j^- h_j m_j$ ,  $\bar{l}'_j = (A_0/A) \sigma \mu_0^+ (1 - h_0) m_j$  and  $\bar{i}'_j = (A_0/A) \sigma \mu_0^- h_0 m_j$ . Thus, the distribution of  $e_{j, n+1}$  will be also a Gaussian distribution with average value

$$\bar{e}_{j, n+1} = a_n m_j \{ \mu_j^+ (1 - h_j) K^+ + \mu_j^- h_j K^- \} + \frac{A_0}{A} \sigma m_j \{ \mu_0^+ (1 - h_0) K_0^+ + \mu_0^- h_0 K_0^- \} \tag{4}$$

and variance

$$\delta_{j, n+1}^2 = a_n m_j \{ \mu_j^+ (1 - h_j) (K^+)^2 + \mu_j^- h_j (K^-)^2 \} + \frac{A_0}{A} \sigma m_j \{ \mu_0^+ (1 - h_0) (K_0^+)^2 + \mu_0^- h_0 (K_0^-)^2 \} \tag{5}$$

since the probabilities of  $l_j$ ,  $i_j$ ,  $l'_j$  and  $i'_j$  are independent of each other.

The probability  $P_j = P_j(a_n, m_j, \sigma, \theta_j)$  that the PSP exceeds a threshold  $\theta_j$  for the  $j$ th marker is now

$$P_j(a_n, m_j, \sigma, \theta_j) = \frac{1}{\sqrt{2\pi}} \int_{x_{j, n+1}}^{\infty} e^{-\frac{x^2}{2}} dx \tag{6}$$

where

$$x_{j, n+1} = \frac{\theta_j - \bar{e}_{j, n+1}}{\delta_{j, n+1}} \tag{7}$$

Equations (4)–(7) with  $\sigma = 0$  are reduced to those derived for isolated netlets in previous work (Fournou *et al.*, 1993).

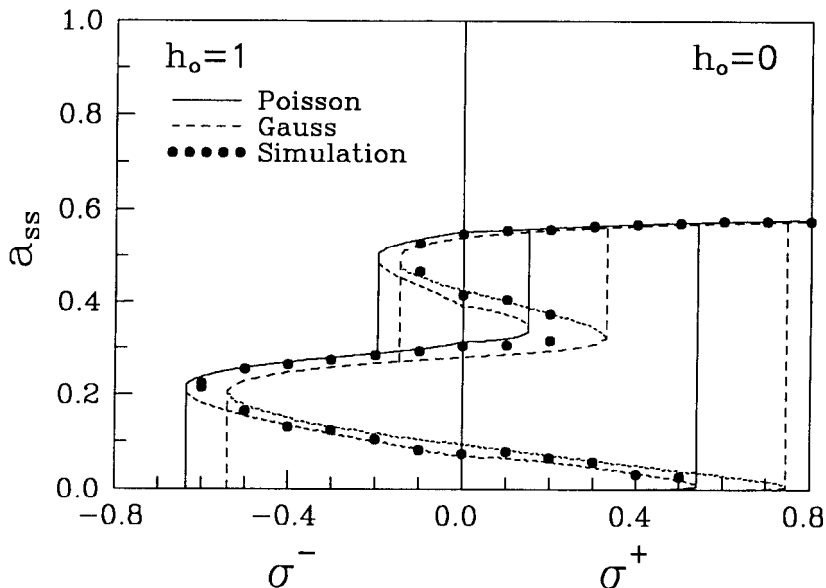


**Figure 1.** Phase diagrams and hysteresis curves for a netlet with two markers,  $a$  and  $b$ , receiving sustained inputs, with  $m_a = 0.7$ ,  $m_b = 0.3$ ;  $\mu_a^+ = 70$ ,  $\mu_b^+ = 80$ ;  $h = 0$ ;  $\theta_a = 23$ ,  $\theta_b = 3$ ;  $r_a = 1$ ,  $r_b = 0$ ;  $K^+ = 1$ ,  $K_0^+ = K_0^- = 0.5$ ;  $\mu_0^+ = \mu_0^- = 10$ . The steady states of activity ( $a_{ss} = a_{Pss}$  for the Poisson approximation and  $a_{ss} = a_{Gss}$  for the Gaussian one) against  $\sigma$  have been plotted. In Poisson curves, the solid lines represent stable steady states and the dashed lines unstable steady states. In Gaussian curves, dashed lines are used for stable steady states and dotted for unstable states. The solid dots are simulation results.

### 2.3. Computer Simulation Model

The theoretical predictions based on the above mathematical formalism may be verified by Monte Carlo computer simulations. With these models, we can produce pictorials of the micro-states of the system at any time, giving us useful insight at the intermediate excitation structures.

The simulation algorithm contains two parts. The first part is concerned with the structure of the network, while the second is devoted to the dynamics of the system. Given the structural parameters of a network of  $A$  neurons and  $N$  markers, the appropriate neuronal connectivity matrix  $[k_{ij}]$  is first constructed. Each element  $k_{ij}$  denotes the synaptic strength of the connection from  $j$  to  $i$  neuron (coupling coefficient). This may take either positive or negative values depending on the type of the synaptic neuron (excitatory or inhibitory, respectively). The threshold  $\theta$  and the other macroscopic parameters ( $K^+$ ,  $K^-$ , or  $\mu^+$ ,  $\mu^-$ ) are considered to vary randomly between a maximum and a minimum value in order to produce more realistic behaviour.

In the second part, the network is activated by specifying the set of neurons which are randomly taken to be active at time  $t = 0$ . One synaptic delay later all neurons linked to them will receive the appropriate inputs. The inputs arriving at a neuron are summed instantly and if the sum exceeds the neuron threshold then the neuron will fire. At the next time step, all active neurons are specified. The

firing neurons for the time step  $t = n\tau$  define the state vector  $a_n$ . Refractoriness of neurons is taken into account by imposing that a neuron that has fired at some moment  $t = n\tau$  cannot fire at  $t = (n + 1)\tau$ .

### 3. Results

Equation (1) with the appropriate expressions of  $P_j$  for each approximation has been used to compute the dynamical properties of netlets with sustained external inputs, for a wide variety of parameters. Some typical results are shown here.

Applying the condition  $\langle a_{n+1} \rangle = a_n$  for steady states of activity (Anninos *et al.*, 1970), we obtained the phase diagrams with two hysteresis loops shown in Figure 1 for a netlet with two markers  $m_a = 0.7$   $m_b = 0.3$ , attached to a cable of afferent fibres which may be axons of  $A_0 = A$  neurons of another netlet. Results for both approximations, Poisson and Gaussian, as well as computer simulation results are depicted in this figure for the sake of comparison. We observe in these plots that the phase diagrams for the Gaussian case is shifted to the right while the Gaussian loops become wider than the Poisson ones. A plausible explanation for this behaviour of the Gaussian nets may be that the larger the value of  $\mu^+$  (making the Gaussian approximation more valid), the larger get to be the memory domains, as it is expected (Anninos & Argyrakis, 1983).

Plots of  $\langle a_{n+1} \rangle$  vs  $a_n$ , for the same netlets as in Figure 1 with  $\sigma = 0$ , are shown in Figure 2. The contribution to the total activity of each one of the two markers is also depicted here. For the chosen set of parameters, we obtain two-modal curves (Adamopoulos & Anninos, 1989) of the total activity, resulting in three stable steady states (the zero level state  $a_{Pss}^0 = a_{Gss}^0 = 0$ , and two no-zero states), and two unstable states.

The computer simulation data in Figures 1 and 2 are in good agreement with the predicted curves. In particular, they are in very good agreement with those of the Gaussian approximation for the region  $a_n \approx 0.4-0.7$ , where there is considerable contribution to the total activity of marker  $a$  with  $\theta_a = 23$  and  $\mu_a^+ = 70$ , which is relatively large.

In Figure 3, we monitor the time course of the total neural activity for the netlet of Figure 1 for several time units (here  $t = 30$ ). Several initial activities are chosen to exhibit as clearly as possible the stable and unstable steady-state levels. We notice in these plots that the Gaussian stable states are always lower than the Poisson ones, while the corresponding Gaussian unstable steady states are higher than those of the Poisson case.

The corresponding time-delay diagrams for the above netlets with the same set of parameters are shown in Figure 4. These diagrams give the time it takes for a netlet to reach a stable steady state as a function of the initial activity. Here, unstable states are represented as 'peaks' and stable steady states as 'wells', but the peak at  $a_0 \approx 0.88$  for the Poisson net (or at  $a_0 \approx 0.82$  for the Gaussian net) is a critical point which controls the time-course behaviour of the netlet for high-level initial activities. If the activity at  $t = 0$  is larger than 0.88 (see Figure 3), then the net will end up in the lower stable steady state,  $a_{ss} \approx 0.31$ , instead of the highest,  $a_{ss} = 0.56$ .

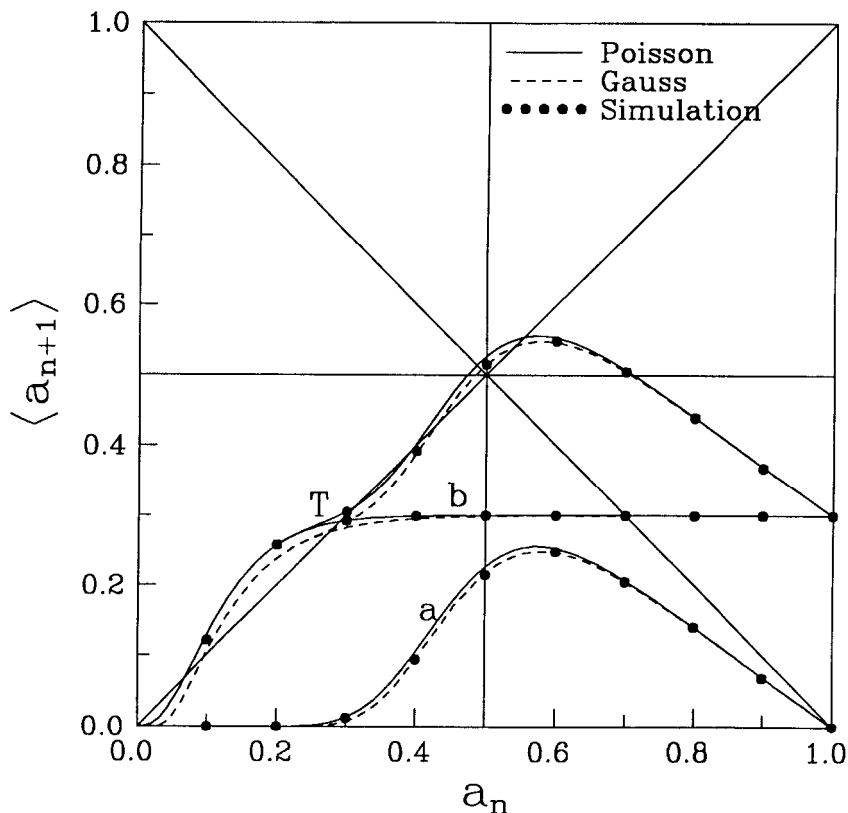


**Figure 2.**  $\langle a_{n+1} \rangle$  vs  $a_n$  for netlet with two chemical markers  $a$  and  $b$ , with  $\sigma = 0$ ;  $m_a = 0.7$ ,  $m_b = 0.3$ ;  $\mu_a^+ = 70$ ,  $\mu_b^+ = 80$ ;  $h = 0$ ;  $\theta_a = 23$ ,  $\theta_b = 3$ ;  $r_a = 1$ ,  $r_b = 0$ ;  $K^+ = 1$ . The curves  $a$  and  $b$  represent the activities of each marker whereas  $T$  gives the total activity of the netlet. Solid lines are used for the Poisson approximation and dashed for the Gaussian one. The solid dots are simulation results.

#### 4. Conclusions

In this paper, we have investigated the effect of the neuronal connectivity on the dynamical behaviour of non-isolated neural nets with chemical markers which receive sustained inputs. We examined the significance and consequences of the replacement of the Poisson by a Gaussian distribution law for the interneuronal connectivity. The calculations in this work, as shown by the analytical formulae (4)–(7) and by the simulation data, provide the opportunity to compare the Gaussian networks with the corresponding Poisson ones. We observed, in general, similar dynamical behaviour in the two approximations, and good agreement between these data and the simulation ones. However, the obtained multiple hysteresis loops were wider for the Gaussian nets than the corresponding Poisson ones, and they had been slightly shifted to larger values of the parameter  $\sigma^+$ , which means more external excitatory sustained inputs. This may be important, as the simple or multiple hysteresis curves (from a functional point of view) may be considered to represent the basis for short-term memory (Harth *et al.*, 1970; Anninos *et al.*, 1970). This trend is justified because nets with large neural

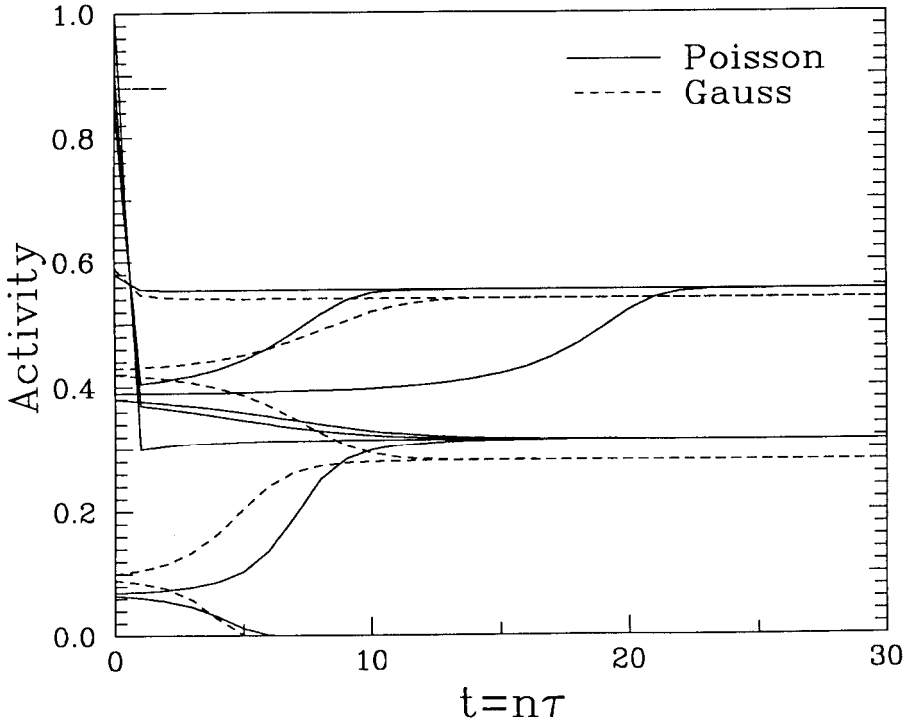


**Figure 3.** Time dependence of total activity  $a_n$  for the netlet of Figure 1 with two markers  $a$  and  $b$ , and  $\sigma = 0$ . Initial activities for Poisson net:  $a_{P0} = 0.065, 0.07, 0.38, 0.39, 0.58, 0.85, 0.9$  and  $1.0$ ; initial activities for Gaussian net:  $a_{G0} = 0.09, 0.1, 0.42, 0.43, 0.59, 0.85, 0.9$  and  $1.0$ . The solid lines are used for the Poisson approximation and the dashed for the Gaussian one.

connectivities follow a Gaussian distribution law for the interneuronal connectivity, whereas nets with small neural connectivities follow the Poisson distribution law (Fournou *et al.*, 1993). Furthermore, in our previous studies, it was stated that the size of the connectivities (value of  $\mu$ ) plays an important role in the width of the hysteresis loops (Anninos & Argyrakis, 1983). In fact it was stated that the larger the value of  $\mu$  the larger is the hysteresis loop, and vice versa. One possible physiological consequence of this is the decay of short-term memory with age. Since old people lose some of their neurons (John, 1967) this implies that some pathways are to be removed. Thus the value of  $\mu$  becomes lower, and the hysteresis loops become narrower. The opposite is true for a young person where the value of  $\mu$  is large, and therefore the hysteresis loops are wider, as in the case of Gaussian neural nets.

Moreover, in the Gaussian nets the stable steady states are lower than the corresponding ones of the Poisson nets, while the unstable states are higher than the corresponding ones of the Poisson nets. These differences depend also on the size of certain structural parameters, mainly the value of  $\mu$ . This parameter must be large enough for the Gaussian approximation to be valid, having as a consequence that the average number of connections (which is the Poisson parameter  $\lambda$ ) is also large (above 50, Cox & Lewis, 1966, p. 21).

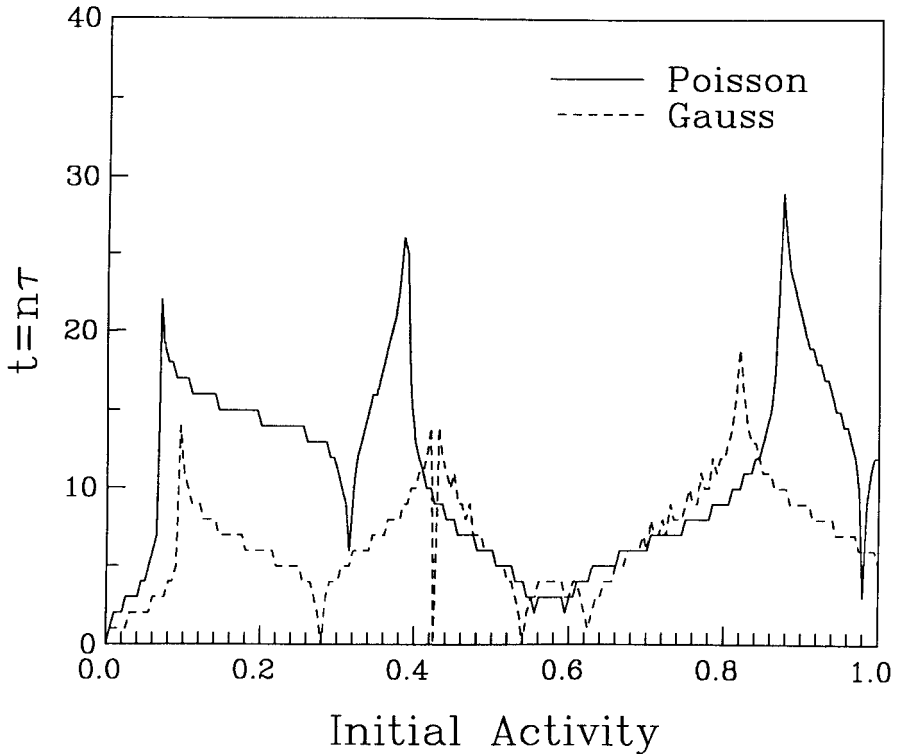


**Figure 4.** Time delay for the netlet of Figure 1 with two markers  $a$  and  $b$ , and  $\sigma = 0$  against the initial activity to reach a stable steady state. The solid lines are used for the Poisson approximation and the dashed for the Gaussian one.

#### Acknowledgement

This project was supported by grant No. E5/1203/1992 of the Ministry of Education (Athens).

#### References

- Adamopoulos, A. & Anninos, P.A. (1989) Dynamic behavior of neural networks with chemical markers. *Connection Science*, **1**, 393–402.
- Anninos, P. & Argyrakis, P. (1983) A mathematical model for the decay of short-term memory with age. *Journal of Theoretical Biology*, **102**, 191–197.
- Anninos, P.A. & Elul, R. (1974) Effect of structure on function in model nerve nets. *Biophysics Journal*, **14**, 8–19.
- Anninos, P.A. & Kokkinidis, M. (1984) A neural net model for multiple memory domains. *Journal of Theoretical Biology*, **109**, 95–110.
- Anninos, P.A., Beek, B., Csermely, T.J., Harth, E.M. & Pertile, G. (1970) Dynamics of neural structures. *Journal of Theoretical Biology*, **26**, 121–148.
- Cox, D.R. & Lewis, A.W. (1966) *The Statistical Analysis of Series of Events*. London: Methuen.
- Fournou, E., Argyrakis, P. & Anninos, P.A. (1993) Neural nets with markers and Gaussian-distributed connectivities. *Connection Science*, **5**, 77–94.
- Harth, E.M., Csermely, T.J., Beek, B. & Lindsay, R.P. (1970) Brain functions and neural dynamics. *Journal of Theoretical Biology*, **26**, 93–120.
- John, E.R. (1967) *Mechanisms of Memory*. New York: Academic Press.
- McCulloch, W.S. & Pitts, W. (1943) A logical calculus of the ideas immanent in nervous activity. *Bulletin of Mathematical Biophysics*, **5**, 115–133.



- Prestige, M.C. & Willshaw, D.J. (1975) On a role for competition in the formation of patterned neural connections. *Proceedings of the Royal Society, Series B*, **190**, 77–98.
- Sperry, R.W. (1943) Visuomotor co-ordination in the newt (*Triturus viridecens*) after regeneration of the optic nerve. *Journal of Comparative Neurology*, **79**, 33–55.
- Sperry, R.W. (1963) Chemoaffinity in the orderly growth of the nerve fiber patterns and connections. *Proceedings of the National Academy of Sciences, USA*, **50**, 703–709.

